




# Analysis of Visual Characteristics of Short-circuited Arc Sites

Seongjun Hong \* and Sun-bae Bang, Department of Safety Research, Korea Electrical Safety Corporation Electrical Safety Research Institute, 111, Anjeon-Ro, Iseomyeon, Wanjugun, Jeollabukdo 55365, Republic of Korea  
Jun-ho Bang, Department of IT Applied Systems Engineering, Jeonbuk National University, 567, Baekje-Daero, Deokjin-Gu, Jeonju-Si, Jeollabuk-Do 54896, Republic of Korea  
Jinyoung Park, Ki-deuk Min and Jin-sik Lee, Department of Safety Research, Korea Electrical Safety Corporation Electrical Safety Research Institute, 111, Anjeon-Ro, Iseomyeon, Wanjugun, Jeollabukdo 55365, Republic of Korea

**Received:** 13 September 2021/**Accepted:** 25 November 2022/**Published online:** 13 December 2022

**Abstract.** Identifying the cause of fire at a fire site is an important fire prevention measure to prevent recurrence. In particular, information about molten marks of the copper wire is essential to check whether electric power is being supplied at the fire site. This study aims to analyse the visual characteristics of arc sites formed by a short circuit to identify the molten marks at the fire site. When a short circuit occurs, electromagnetic force is generated by the short circuit current, and the arc repulsion force is generated by the contact arc. In this study, the effects of the forces, which act on the short-circuited melted area, on the formation of copper molten marks were investigated. Copper molten marks formed by a short circuit were experimentally fabricated, and the visual characteristics based on the force that was applied to the melted area were identified and classified based on features. The results showed that the melted area was affected by both the arc repulsion and electromagnetic forces, resulting in the visual differences between the short-circuited arc sites and flame-melted ones, which are affected by gravity and molecular force. These results provide a theoretical basis for discriminating between arc sites formed by a short circuit and flame-melted marks at the fire site. The validity of this study was verified via a comparative analysis using shape and cross-sectional microstructure of molten marks collected at the fire site.

**Keywords:** Copper wire, Arc site, Arc melting, Globule, Arc bead, Melting mark shape, Short circuited melting mark

## 1. Introduction

Short circuits are a cause of electrical ignition, and they melt copper wire and create arc sites. Fire investigators use arc sites as clues to distinguish an electric fire. Therefore, it is critical to accurately examine the arc sites to assist the investigator

---

\*Correspondence should be addressed to: Seongjun Hong, E-mail: shanks0221@gmail.com



in determination of both the origin and cause of fire, and establish preventive measures. Currently, fire investigators investigating the cause of fires are using the guidelines described in NFPA-921 (2021) [1] and Electrical Fires and Explosions (2021) [2] to distinguish melting marks by a short circuit and flame at the scene of a fire.

The analysis of visual characteristics, a relatively simple technique that can easily be conducted on-site, is employed to distinguish only between melting marks due to a short circuit and those due to flame at a fire scene, which can increase work efficiency [3–5]. In 1971, the Tokyo Fire Department Fire Investigation Division conducted an external analysis of the colour, lustre, and shape between the cause beads and the victim beads [4]. The report concluded that the boundary between the melted beads was not clear although the primary melted beads tended to be glossier and have fewer black spots on the surface than the secondary melted beads. Benfer and Gottuk [5] analysed receptacles with fire-induced arcing and proposed that resolidification waves, spatter, localized damage with a sharp line of demarcation, and corresponding damage on the opposing conductor were evident characteristics of arc-generated marks. Moreover, seven characteristics of short-circuited arc sites and five of flame-melted marks were listed in the “Visual Characteristics of Fire Melting on Copper Conductors” report published by the ATF Fire Research Laboratory [3]. These characteristics were based on the National Fire Protection Association’s (NFPA’s) publication, the “Guide for Fire and Explosion Investigations (NFPA 921)”, which is continuously updated regarding the visual characteristics of melted beads formed by short circuits, ground faults, and poor contact [1]. A recent study explained the characteristics of short-circuited melted beads and flame-melted marks obtained from fire sites in detail and proposed a methodology for the identification of damage on electrical wiring [6]. Nevertheless, previous studies that have analyzed the visual characteristics of arc sites have only focused on a small number of samples collected from the fire site that focuses on short-circuits, failing to extract the fundamental characteristics of arc sites formed in various locations and situations.

This study aims to analyse the visual characteristics of arc sites for a rapid assessment of the copper melting marks at the fire site. This paper comprises five

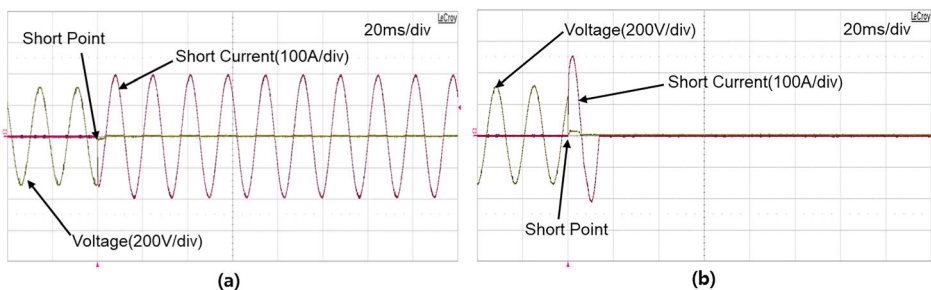


**Figure 1. Short circuit current waveform from AC220V voltage source. (a) Short circuit current of 150 A or less; (b) Short circuit current greater than 150 A.**

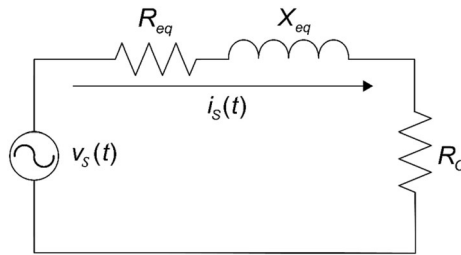


**Figure 2. Equivalent circuit of the short circuit in the distribution line.**

sections starting with the introduction. Section 2 investigates the forces acting on the melted area during the straight, parallel, and cross-contact of copper wires and analyses the effect of the forces on the formation of copper melting marks formed by a short circuit. In Sect. 3, the formation of the short-circuited arc sites is presented, and the external features are analysed using the wire contact angle, wire type, voltage, and ambient temperature as variables. Section 4 presents a comparative analysis between the characteristics of the arc sites analysed in Sect. 3 and those collected from the fire sites. Finally, Sect. 5 concludes the paper.

## 2. Characteristics of the Short-circuited Arc Site Formation

### 2.1. Characteristics of Short Circuit Current Distribution System

A short circuit occurs when an energized conductor touches a grounded conductor or a grounded metal object with low circuit resistance, thereby causing a large surge current in the circuit [1]. The electrical flow is completed via a shorter route than the established wiring. Generally, most houses employ a voltage of AC 110 V to 220 V. The short circuit current is dependent on the transformer capacity and impedance of the distribution system, and is controlled by protective devices, such as circuit breakers. The short circuit current and contact resistance result in Joule heating, as expressed in Eq. 1. The Joule heating often melts the circuit components at the fault location.

$$H = I_S^2 \times R_C \times t_C, \quad (1)$$

where  $H$  is the Joule heating (J),  $I_S$  is the short circuit current (A),  $R_C$  is the contact resistance ( $\Omega$ ), and  $t_C$  is the short circuit time(s). Figure 1 shows the waveform of the short circuit current generated when a  $1.5 \text{ mm}^2$  copper wire is short-circuited in a building with an AC 220 V distribution voltage. The wire melts and welds due to Joule heating when wires with a potential difference are in contact at a short circuit current of 150 A or less, and a short circuit current occurs until the circuit breaker operates as shown in Fig. 1a. The contact area of the entire wire melts and splashes at the short circuit current that exceeds 150 A. A short circuit

current is formed for a short period of 0.5 to 1.5 cycles because the wires are out of contact at this time, as shown in Fig. 1b.

Figure 2 shows the diagram of the equivalent circuit of a short circuit inside a general building. A large short circuit current  $i_S(t)$  is instantaneously generated when a short circuit occurs between wires, as expressed in Eq. (2).

$$i_S(t) = \frac{v_S(t)}{R_{eq} + X_{eq} + R_C}, \quad (2)$$

where  $v_S(t)$  is the power supply voltage (V),  $R_{eq}$  is the equivalent line resistance ( $\Omega$ ),  $X_{eq}$  is the equivalent line reactance ( $\Omega$ ), and  $R_C$  is the contact resistance ( $\Omega$ ). When a short circuit current flows because of the contact between wires in the distribution line, the contact area of the copper wire is melted by Joule heating.

## 2.2. Forces Acting on the Melted Area During Short Circuit

When an arc occurs, temperatures of more than 3000°C are generated at the point of contact between the wires because of arc and Joule heating [2], which exceeds the melting point of copper wires (1084°C). It is difficult to model the effect of all the forces on the formation of the arc site because of the complex geometry of the short circuit point. However, the surge of the current generated when a short circuit occurs increases the electromagnetic force, and the arc at the contact area generates the arc-repulsion force. These two forces have the potential to influence the shape of the arc site produced when a short circuit occurs. Equation (3) expresses the force that the molten portion of a conductor is subjected to when a short circuit occurs.

$$\vec{F}_S = \vec{F}_L + \vec{F}_A \quad (3)$$

where  $F_S$  is the force acting on the wire contact area during the short circuit,  $F_L$  is the electromagnetic force, and  $F_A$  is the arc repulsion force. The shape of the wire, which melts because of the short arc, is changed by the force acting on the melted area,  $F_S$ , exhibiting different visual characteristics from the flame-melted mark, which are mainly affected by gravity and molecular force.

**2.2.1. Electromagnetic Force Generated During Short Circuit** In the event of a short circuit, the contact part of the energized wires is subjected to the electromagnetic force generated caused by the short circuit current flowing through the two conductors, and it can be expressed as Eq. (4) [7–11].

$$F_L = F_{Line\_A} + F_{Line\_B}, \quad (4)$$

where  $F_{Line\_A}$  and  $F_{Line\_B}$  are the electromagnetic forces acting on the contact area.  $F_{Line\_A}$  and  $F_{Line\_B}$  can be expressed as Eq. (5) [11].

$$F_{Line\_A}, F_{Line\_B} = I_S I_S B_S \sin\theta, \quad (5)$$

where  $I_S$  is the short circuit current flowing through the conductor,  $B_S$  is the magnetic flux density created by the short circuit current,  $l_S$  is the length of the contact area, and  $\sin\theta$  is the sine of the angle between the magnetic field and the current flowing through the contact area. Moreover, the magnetic flux density,  $B_S$ , can be obtained as in Eq. (6).

$$B_S = \mu_0 \mu_S H_S, \tag{6}$$

where  $\mu_0$  is the permeability of free space,  $\mu_S$  is the relative permeability, and  $H_S$  is the magnetic field generated by the short circuit current. The strength of the magnetic field can be expressed as in Eq. (7).

$$H_S = \frac{I_S}{4\pi r}, \tag{7}$$

where  $r$  is the distance between the melted area and the center of the lead wire. The electromagnetic force that acts on the melted area can be calculated using Eq. (8)

$$F_L = \mu_0 \mu_S l_S \frac{I_S^2}{2\pi r} \sin\theta \tag{8}$$

2.2.2. *Arc Flash Force* A contact arc is generated at the micro-contact area with arc pressure higher than the atmospheric pressure when wires with a potential difference are in contact. The force acting on the contact area is called the arc repulsion force, and the force causes the melted copper wire splashes in all directions because of Joule heating. Equation (9) expresses the arc repulsion force from the energy equilibrium equation [12–14].

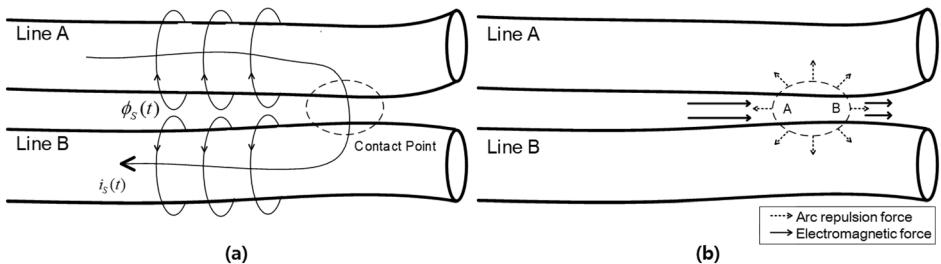


**Figure 3. Directions of the magnetic flux and force generated when parallel lead wires are short circuited. (a) Short circuit current and magnetic flux generated during short circuit; (b) Forces acting on melted area.**

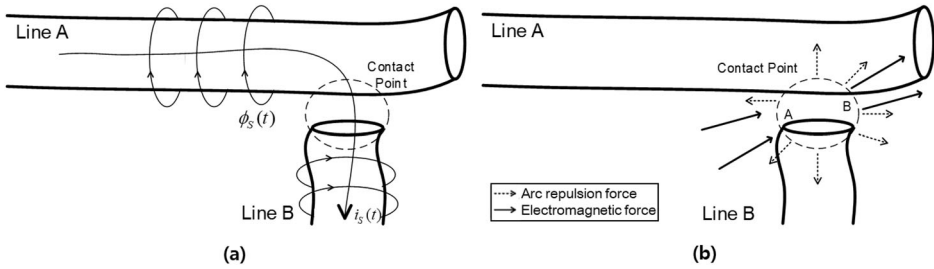


**Figure 4. Directions of the generated magnetic flux and force when crossing lead wires are short circuited. (a) Short circuit current and magnetic flux generated during short circuit; (b) Forces acting on the melted area.**

$$F_A = 2 \frac{\eta I_S V_S A}{\epsilon_0 A_a \delta} \tag{9}$$

where  $\eta$  is the percentage of the energy and assuming 70% due to radiation,  $I_S$  is the current flowing through the lead wire when an arc occurs,  $V_S$  is the voltage difference between the lead wires when an arc occurs,  $A$  is the cross-sectional area of the arc,  $A_a$  is the contact area between lead wires, and  $\epsilon_0$  is the plasma emission coefficient at atmospheric pressure.

**2.3. Forces Acting on the Melted Area Based on the Position of the Wires During Short Circuit**

When two energized wires come into contact with each other and a short circuit occurs, it is assumed that the electromagnetic and arc repulsion forces act according to Eq. (3) on the contact part. Unlike the arc repulsion force that acts in all directions at the point of contact of the wires, the direction of the electromagnetic force is determined by the path of the short circuit current. Through Cases 1, 2,

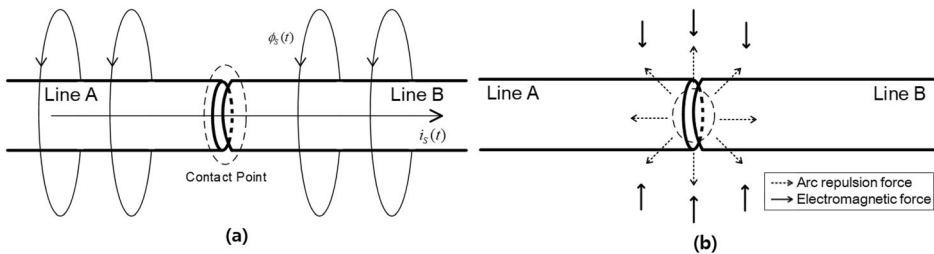


**Figure 5. Directions of the magnetic flux and force generated when lead wires placed in a straight line are short circuited. (a) Short circuit current and magnetic flux generated during short circuit; (b) Forces acting on the melted area.**

and 3, the direction of the force acting on the contact area was predicted according to the contact location of the physical wire.

**2.3.1. Case 1** Figure 3 shows the magnetic field generated by the short circuit current and the forces acting on the contact area when two wires (Lines A and B), which are placed side by side in parallel, with a potential difference, come into contact. Subsequently, the magnetic flux  $\phi_s(t)$  is generated along the path where the short circuit current flows, as shown in Fig. 3a. A repulsive force between the two parallel lead wires is generated to repel each other momentarily, and the electromagnetic force acts on the contact area of the two wires where the magnetic flux line is weak, as shown in Fig. 3b. Moreover, the magnetic flux generated by the short circuit of the parallel lead wires is obtained in the similar direction between the wires, and it amplifies the electromagnetic force acting on the melted copper in the contact area. The magnetic flux and the current flowing at the point of contact form an angle of 90 degrees. The repulsive force generated by the arc flash acted in all directions at the contact area. The electromagnetic and the arc repulsion forces in the contact area shown in Fig. 3b, cancel each other at point A, which is the power side, and combine at point B, which is the load side, thereby affecting the shape formation.

**2.3.2. Case 2** Figure 4 show the magnetic field generated by the short circuit current and forces acting on the contact area when two wires (Line A and Line B) with a potential difference come into contact at a right angle. The magnetic flux  $\phi_s(t)$  is generated in the direction shown in Fig. 4a along the path where the short circuit current flows. The magnetic flux and the current flowing at the point of contact form an angle of 45 degrees. The electromagnetic force acts on the contact area of the two wires where the magnetic flux line is weak, as shown in Fig. 4b. Additionally, the electromagnetic and arc repulsion forces in the contact area, as

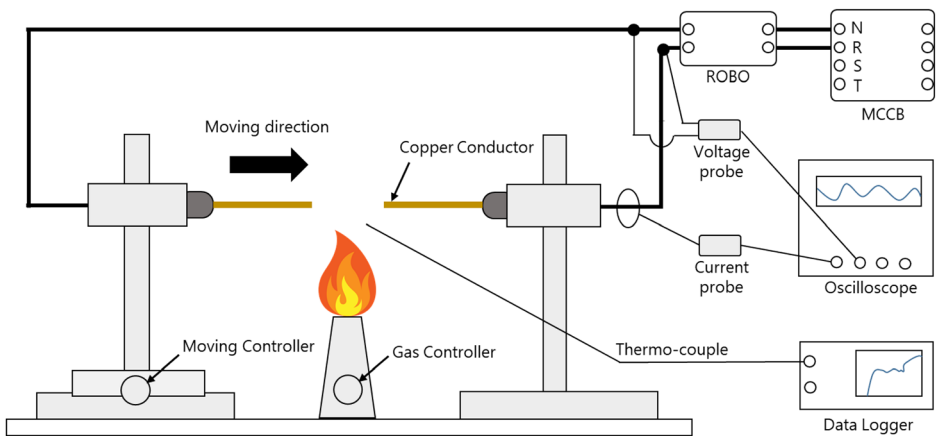


**Figure 6. Configurations for arc site fabrication.**

shown in Fig. 4b, cancel each other at point A and combine at point B, thereby affecting the shape formation.

**2.3.3. Case 3** Figure 5 shows the magnetic field generated by the short circuit current and the forces acting on the contact area when two wires (Line A and Line B) with a potential difference that are placed in a straight line come into contact. Subsequently, the short circuit current flows and magnetic flux  $\phi_S(t)$  are generated in the clockwise direction when wires with a potential difference are contacted, as shown in Fig. 5a. The magnetic flux and the current flowing at the point of contact form an angle of 0 degrees. The electromagnetic force acts towards the centre of the lead wire and the melted area caused by the generated magnetic field. Meanwhile, the repulsive force due to the electric arc at the contact area is generated in all directions, as shown in Fig. 5b.

### 3. Fabrication of Short-circuited Arc Sites and Analysis of Visual Characteristics

The analysis of the characteristics of short-circuited arc sites collected at the fire site have several limitations. The short-circuited arc sites collected at the fire site do not indicate the exact conditions at the time of formation. Moreover, extracting the visual characteristics of these arc sites is difficult because of the presence of corrosion and the adhesion of foreign substances. On the other hand, the experimentally formed short-circuited arc sites indicate the experimental conditions, and the correlation between the experimental conditions and the characteristics of the arc sites is obtained by extracting the characteristics of the arc sites generated under each experimental condition. In the experiment, short-circuited arc sites were produced by changing the type of wire, location of wire, and ambient temperature. The effect of continued fire impingement after the arc site was created was not explored.

#### 3.1. Fabrication of Short-circuited Arc Sites

The shapes of short-circuited arc sites at fire sites and the environment where they are formed are diverse and varied. Various experimental conditions were used to

**Table 1**  
**Specifications of MCCB and ROBO**

Device type	Model	Maker	Pole	Rated current	Instantaneous tripping type	Acquisition standard
MCCB	ABS104c-K	LS Electric	4	100	C type (Class 20)	IEC60898
ROBO	32GRhN-K	LS Electric	2	20	C type (Class 20)	IEC61009



**Table 2**  
**Experimental Matrix for Making Arc Sites**

Exp #	Ambient temperature (°C)	Source voltage (Vrms)	Location of wire	Core type	Wire thickness (mm <sup>2</sup> )	Number of trial attempts
1-1	25	AC 220	Case-1	Single-strand	4	2
1-2	25	AC 220	Case-2	Single-strand	4	2
1-3	25	AC 220	Case-3	Single-strand	4	2
2-1	25	AC 220	Case-1	Concentric-stranded	4	2
2-2	25	AC 220	Case-1	Cord wire	4	2
3-1	25	AC 380	Case-1	Single-strand	4	2
4-1	900	AC 220	Case-1	Single-strand	4	2
4-2	900	AC 220	Case-2	Concentric-stranded	4	2
4-3	900	AC 220	Case-3	Cord wire	4	2

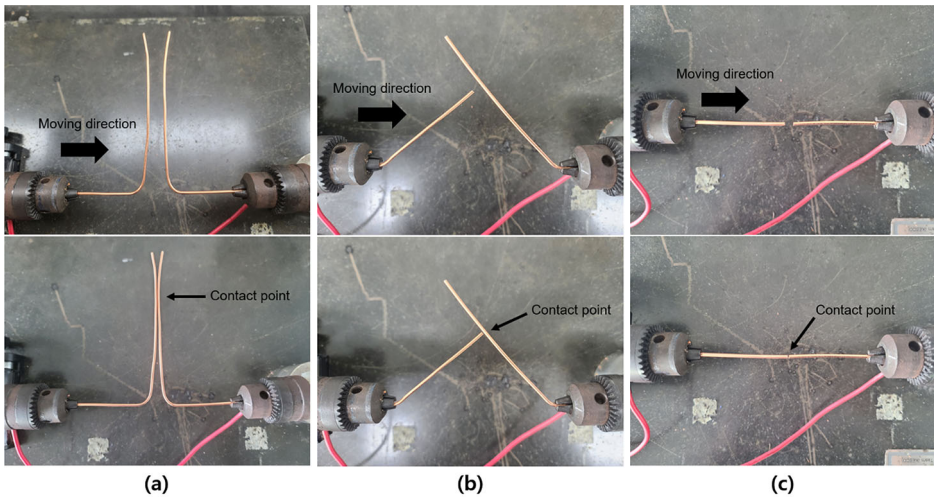


**Figure 7. Configurations for arc sites fabrication (a) Wire location of Case-1; (b) Wire location of Case-2; (c) Wire location of Case-3.**

represent the short circuit environments that were likely to occur at fire sites. To create the arc sites, a short circuit was created with copper conductors.

Figure 6 shows the configuration for arc site fabrication. The fixed copper wire was contacted using a moving controller. The power connected to the copper wire

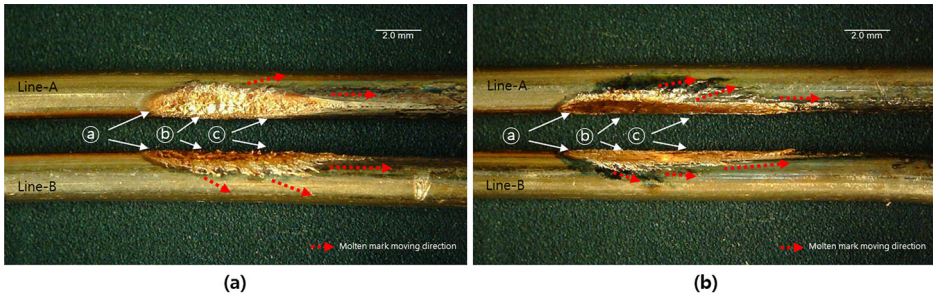


**Figure 8. Arc sites produced in Experiment 1-1, (a) Arc site 1-1(1); (b) Arc site 1-1(2).**

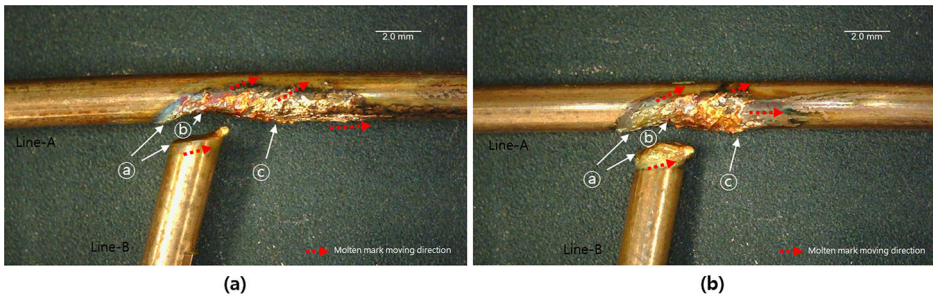


**Figure 9. Arc sites produced in Experiment 1-2. (a) Arc site 1-2(1); (b) Arc site 1-2(2).**



**Figure 10. Arc sites produced in Experiment 1-3. (a) Arc site 1-3(1); (b) Arc site 1-3(2).**

was at AC 220 V or 380 V, and the ambient temperature of the contact area was controlled through a gas controller. In the event of a short circuit, the current and voltage were measured using an oscilloscope (WaveRunner 6Zi), and the temperature of the wire contact area was measured using a data logger (LR8402) and thermocouple (K-type). Molded case circuit breaker (MCCB) and residual current operated circuit breaker with integral overcurrent protection (RCBO) were used

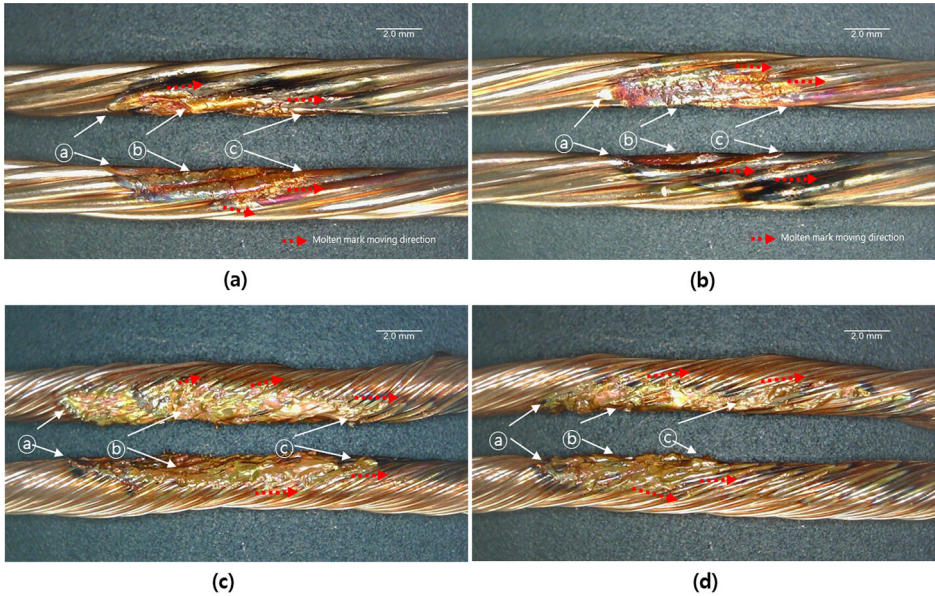


**Figure 11. Arc sites produced in Experiments 2-1 and 2-2. (a) Arc site 2-1(1); (b) Arc site 2-1(2); (c) Arc site 2-2(1); (d) Arc site 2-2(2).**

for protection relay. The MCCB (ABS52c-K) used in the experiment trips when overload or short circuit occurs. RCBO (32GRhN-K) trips when overcurrent, short circuit, or leakage occurs. Table 1 listed the specifications of the MCCB and ROBO.

Table 2 shows the experimental matrix for the fabrication of arc sites. Experiments 1-1, 1-2, and 1-3 were conducted to confirm the direction of the force acting on the wire contact area and the shape of the arc site according to the physical location of the wire. For the position of the electric wire, three cases of parallel contact (Case-1), perpendicular contact (Case-2), and straight contact (Case-3) were tested. Figures 7a–c show the wire positions in Case-1, Case-2, and Case-3, respectively. As shown in Fig. 7, in each case, the copper wire was contacted using a moving controller. The single-strand wire, which is the simplest type of wire, was used.

Experiments 2-1 and 2-2 were conducted to confirm the difference in arc sites according to the core-type of copper wire. In Experiments 2-1 and 2-2, a concentric stranded wire consisting of 7 inner core wires and a cord wire consisting of a bundle of  $0.1 \text{ mm}^2$  thick core wires were used, respectively.

Experiment 3-1, as shown in Table 2, was conducted to confirm the difference in the short-circuited arc sites according to the change of the power-supply voltage. Experiment 3-1 used a voltage of AC 380 V to produce an arc site, and for comparison, Experiment 1-1 was conducted at AC 220 V. Among the standard voltages currently defined in IEC-60038, the voltage of AC 230/400 V exists. However, AC 220/380 V and AC 240/415 V systems still exist in some countries.

The laboratory in which the arc site manufacturing experiments were conducted is located in an area employing a 220/380 V system, and the voltage transfer was not coupled to avoid creating additional impedance. Moreover, because wires are usually wired in parallel, the experiment was conducted under Case-1 situation.

Experiments 4-1, 4-2, and 4-3, as shown in Table 2, were performed to confirm the morphological difference according to the ambient temperature when generating a short-circuited arc site. A short circuit was created while the flame was applied to the electric wire, and, referring to the report of Weinschenk et al., the flame was maintained for 2 min before and after the short circuit. In addition, the ambient temperature of the wire contact area was maintained at approximately 900°C using a gas controller [15].

### 3.2. Experimental Results

*3.2.1. Shape of Arc Site According to the Physical Location of the Wire and Direction of the Force Acting on the Wire Contact Area* Figures 8, 9, and 10 show the results of Experiments 1-1, 1-2, and 1-3 shown in Table 2, respectively. The experiments were conducted 25°C, which is the room temperature, and two repetitions of each experiment were performed by applying an AC 220 V voltage. In Experiment 1-1, a short-circuited arc site was fabricated by placing the copper wire ener-

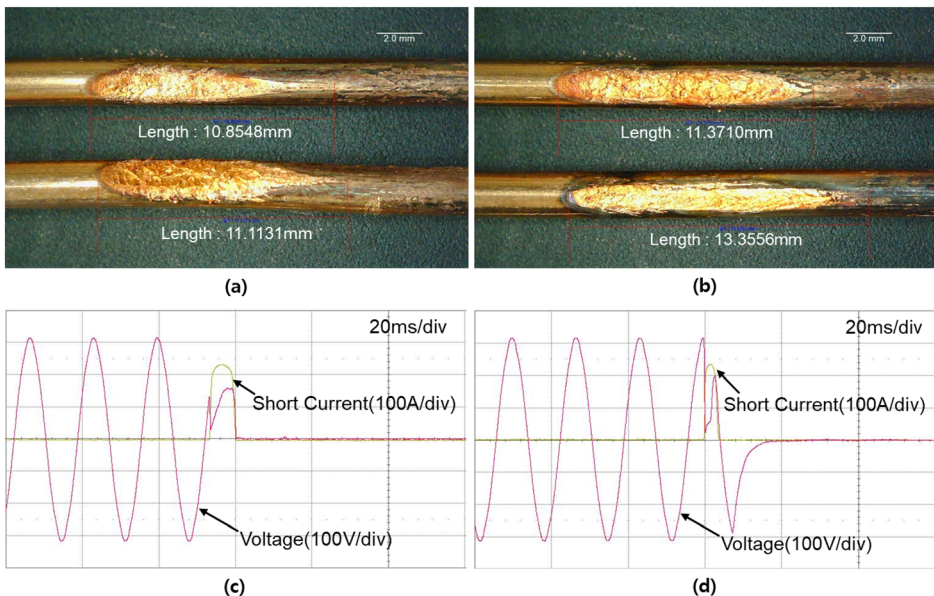


**Figure 12. Arc sites generated from AC 220 V voltage and electrical waveforms. (a) Major axis length of melt mark 1-1 (1); (b) Major axis length of melt mark 1-1 (2); (c) Electrical waveform when generating arc site 1-1 (1); (d) Electrical waveform when generating arc site 1-1 (2).**

gized in parallel and moving it through the moving controller of the experimental device. The arc sites fabricated in Experiment 1-1 were divided into parts (a), (b), (c), as shown in Figs. 8a and b. Part (a) is on the power-source side, part (c) is opposite to the power source, and part (b), with the deepest indentation, is the contact point of the two wires. In part (a), the molten copper did not invade the area with the adjacent un-melted copper wire; therefore, the boundary of arc site can clearly be identified. Parts (a) and (b) are thinly coated with melted copper. When viewed from the contact area (b), the arc site distribution range is wider in the direction of part (c) than in part (a). In addition, the overall shape of the arc sites 1-1 (1) and 1-2 (2) extends from part (a) to part (c), and the arc sites in part (c) invade over the un-melted wire surface and are solidified. The direction from part (a) to part (c) coincides with the direction of the electromagnetic force. Furthermore, when considering the direction of the arc site extending diagonally, the influence of the arc repulsion force acting in all directions at the contact point is identified.

In Experiment 1-2, a short-circuited arc site was fabricated by placing a copper wire energized vertically and moving it through the moving controller. The arc sites produced in Experiment 1-2 were divided into parts (a), (b), and (c), as shown in Figs. 9a and b. Part (a) is on the power source side, part (b) is where the wire-to-wire contact occurs, and part (c) is the side opposite the power source. As in the case of Experiment 1-1, the boundary between the molten and non-mel-

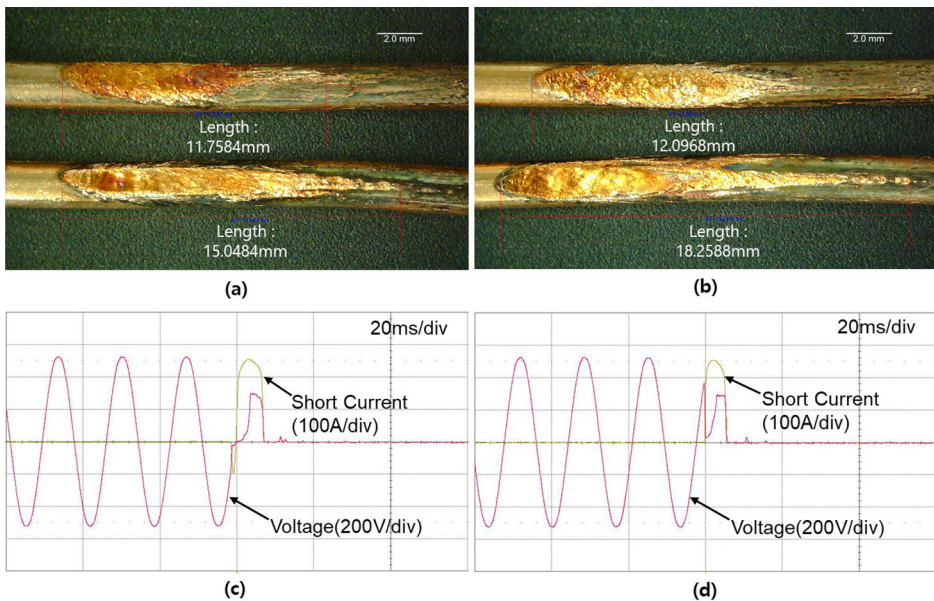


**Figure 13. Arc sites generated from AC 380 V voltage and electrical waveforms. (a) Major axis length of arc site 3-1 (1); (b) Major axis length of arc site 3-1 (2); (c) Electrical waveform when generating arc site 3-1 (1); (d) Electrical waveform when generating arc site 3-1 (2).**

ted regions can clearly be observed in part (a). In addition, when viewed from the contact area (b), the arc site distribution range is wider in the direction of part (c) site than in the direction of the (a) site. The overall arc site has a shape extending from part (a) to part (c). In particular, part (c) is located in the direction opposite to the current flowing path, and the shape of the arc site covered over the un-melted wire can be observed. In Experiment 1-2, as in 1-1, it was observed that the direction of force was from part (a) to part (c).

In Experiment 1-3, a short-circuited arc site was fabricated by placing the powered copper wires in a line and moving the wires through the moving controller. Figures 10a and b show the arc sites produced in Experiment 1-3, and part (a) shows the part where the wire-to-wire contact occurred. The influence of the arc repulsion force acting in all directions can be identified in the shapes of the arc sites 1-3(1) and 1-3(2). Arc sites 1-3(1) and 1-3(2) have a shape that spreads out without a specific direction around the contact point (a). In addition, owing to the effect of arc repulsion, the molten copper wire invades and solidifies on the surface of the adjacent un-melted copper wire.

*3.2.2. Effect of Wire Core Type on Arc Site Experiments 2-1 and 2-2* shown in Table 2 were performed to confirm the morphological difference of the arc site according to the wire core type. Experiments 2-1 and 2-2 were conducted using concentric-stranded and cord wires under the experimental conditions same as those in Experiment 1-1. Figures 11a and b show the arc sites produced in Experiment 2-1, and Figs. 11c and d show the arc sites produced in Experiment 2-2. The arc sites produced in Experiments 2-1 and 2-2, as shown in Fig. 11, were divided into parts (a), (b) and (c) similar to the arc site produced in Experiment 1-1, and each part has similar characteristics. In part (a), the boundary of the arc site can clearly be identified. In addition, the overall arc site has a shape extending from

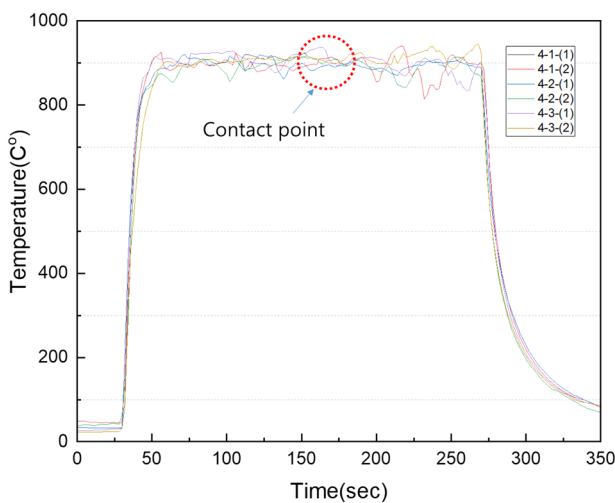


**Figure 14. Ambient temperature flux of wire contact area.**

part (a) to part (c), and the arc site in part (c) invades over the un-melted wire surface.

**3.2.3. Effect of Voltage Difference on Arc Site** To observe the variations in the arc sites caused by a difference in power-supply voltage, an arc site was fabricated by the method used in Case-1 using an AC voltage of 380 V, as in Experiment 3-1 shown in Table 2. Furthermore, for comparison, the arc site produced in Experiment 1-1 shown in Table 2 was used. Figures 12a and b display the arc sites 1-1(1) and 1-1(2) produced at AC 220 V. The major-axis lengths of arc site 1-1(1) were approximately 10.85 mm and 11.11 mm, and the major axis lengths of 1-1(2) were measured to be approximately 11.37 mm and 13.35 mm. Figures 12c and d show the voltage and current waveforms measured during the production of arc sites 1-1(1) and 1-1(2), respectively. The maximum value of the short circuit current was 232 A and 231 A, respectively, and the duration of the short circuit was measured to be 8 ms and 4 ms, respectively. After the short circuit current occurred, the power-supply was cut off by the operation of the protective relay. Figures 13a and b display the arc sites 3-1(1) and 3-1(2) produced at AC 380 V. The major axis lengths of the arc site 3-1(1) were approximately 11.75 mm and 15.04 mm, and the major axis lengths of the arc site 3-1(2) were measured to be approximately 12.09 mm and 18.25 mm. Figures 13c and d show the voltage and current waveforms measured during the fabrication of arc sites 3-1(1) and 3-1(2). The maximum values of the short circuit current were 253 A, 251 A, respectively, and the duration of the short circuit was measured to be 8.4 ms and 6.8 ms, respectively. After the short circuit occurred, the power-supply voltage was cut off by the operation of the protective relay. Figures 13 and 14 shows that the overall shapes of the arc sites produced at AC 220 V and 380 V are similar. However, the maximum short circuit current was 20 A greater with the higher power supply voltage. In addition, the average major axis length of the arc site produced under AC 220 V condition was 11.67 mm, and the average major axis length of the arc site produced under AC 380 V condition was calculated to be 14.28 mm. A difference of 2.61 mm occurred in the average major axis length of the arc site, which is

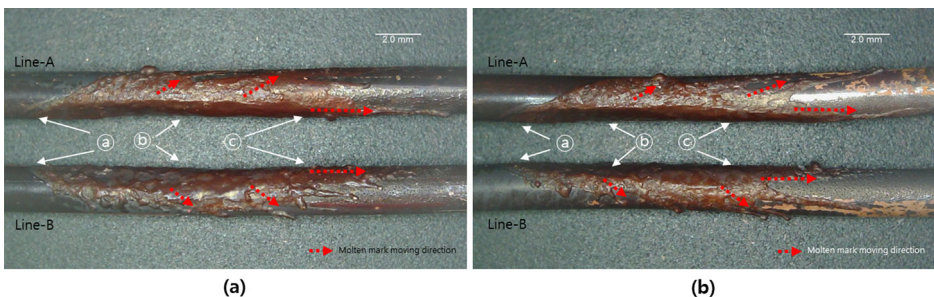


**Figure 15. Arc sites produced in Experiment 4-1. (a) Arc site 4-1(1); (b) Arc site 4-1(2).**

considered to be influenced by the increase in the arc repulsion and electromagnetic forces due to the increase of the short circuit current.

*3.2.4. Effect of Ambient Temperature on Arc Site Experiments 4-1, 4-2, and 4-3* listed in Table 2 were performed to confirm the morphological difference of the arc site according to the temperature difference. Figure 14 shows a graph of the temperature measured in the process of making a total of six arc sites in Experiments 4-1, 4-2, and 4-3. Heating was performed for approximately 2 min before and after the short circuit occurred.

Figure 15 shows the experimental results of Experiment 4-1. The arc site produced in Experiment 4-1 can be divided into parts (a), (b) and (c) as with the arc site in Experiment 1-1, and they show a similar shape extending from part (a) to part (c). The arc sites produced in Experiment 4-1 showed a melting area wider than those of the arc sites produced in Experiment 1-1. In particular, the arc sites are widely distributed up to the opposite side of the contact area (b).

Figure 16 shows arc sites 4-2(1) and 4-2(2) produced in Experiment 4-2. In arc site 4-2(1) shown in Fig. 16a, compared with the samples of Experiment 1-2 (Fig. 9), the interface of part (a) can more clearly be distinguished, and the contact part (b) is deeper. Moreover, arc site 4-2(1) maintains the direction from (a) to (c), as in Experiment 1-2, and is widely distributed on sides of part (b), which is the contact part. Figure 16b shows arc site 4-2(2) produced in Experiment 4-2. In Fig. 16b, Line-A is melted and separated into Line-A(1) and Line-A(2). Parts (a) and (c) in Fig. 16b maintain shapes similar to parts (a) and (c) in Fig. 16a, but part (b) is molten. At the separated point of Line-A(1), a molten bead is formed as shown in part (d). Moreover, as shown in (e), a drawing line connected to the molten bead is observed. Line-B in Figs. 16a and b is completely covered with melting marks, and it can be identified that the drawing line develops in the direction opposite to the power source.

Figure 17 shows the experimental results of Experiment 4-3. As with the arc sites generated in Experiment 1-3, the arc sites generated in Experiment 4-3 have a shape that spreads out in all directions around part (a), without a specific direc-

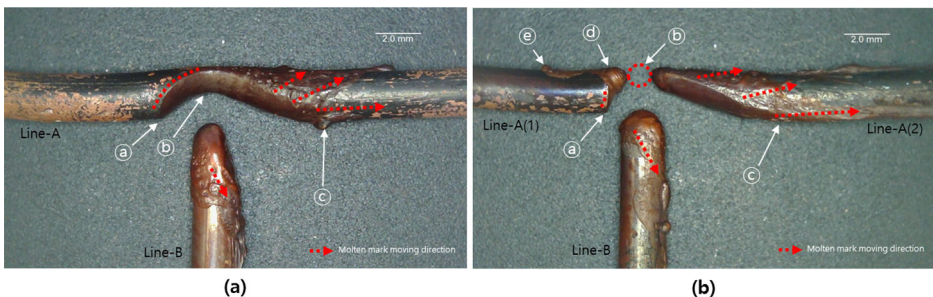


**Figure 16. Arc sites produced in Experiment 4-2. (a) Arc site 4-2(1); (b) Arc site 4-2(2).**



tion. In addition, the arc site produced in Experiment 4-3 showed a melting area wider than that in Experiment 1-3.

The characteristics of the arc sites shown in Figs. 15, 16, and 17 are similar to those of the arc sites in Figs. 7, 8, and 9, respectively. This is suggested to be the result of the forces acting in the same direction at the contact area. However, a more dynamic shape was observed in the arc site generated at 900°C than that generated at 25°C, which is suggested to be a result of more melting at the contact area when a short circuit occurs at the higher temperature.

### 3.3. Summary

In the experiments performed under the conditions of Cases 1 and 2, the shape of the short circuit arc site showed a common characteristic affected by the electromagnetic and arc repulsion forces. In the experiments performed under the conditions of Cases 3, the shape of the short-circuited arc site showed a common characteristic affected by arc repulsion forces. The shape of the short-circuited arc site had three common characteristics based on the electromagnetic and arc repulsion forces. The first characteristic is shown in part (a) of Figs. 8, 9, 11, 14, and 15. Part (a) formed on the power side in the form of a ramp edge, and the boundary can clearly be identified because the melting copper does not invade the un-melted part. Ramp-edge form is often found in short-circuited arc sites where the contact part of the wire is dented due to short circuit; and this form was also observed on the power supply side of the wire separated due to the short circuit as in Line-A(1) of Fig. 15b. Moreover, the shape of the ramp edge can often form an arc site with the bead as shown in part (b) in Fig. 15b. The second characteristic is the covered form shown in the part (c) in Figs. 8, 9, 11, 15, 16. The covered form refers to the type in which the melting copper is spread over the surface of the un-melted wire. The covered form is also often found in concave shaped arc sites; and it was also observed in separated wires as in Line-A(2) in Fig. 16b. The third characteristic is the concave shape. The concave shape is shown in Figs. 8, 11, 15 and Line-A in Figs. 9 and 16a. The concave shape includes the ramp edge form on the power-supply side and the covered form on the side opposite to the power-supply side. These three characteristics are expected to be influenced by the

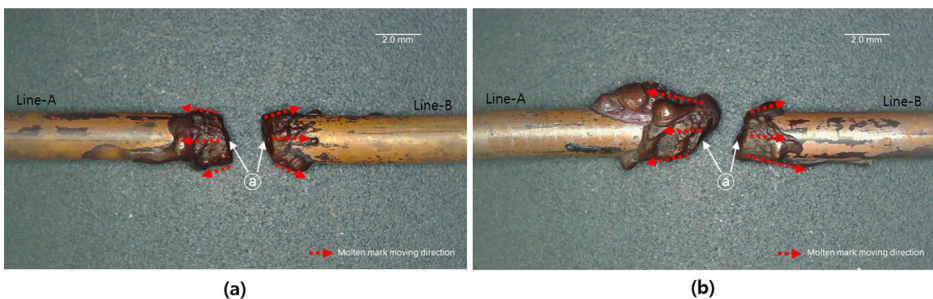


**Figure 17. Arc sites produced in Experiment 4-3. (a) Arc site 4-3(1); (b) Arc site 4-3(2).**

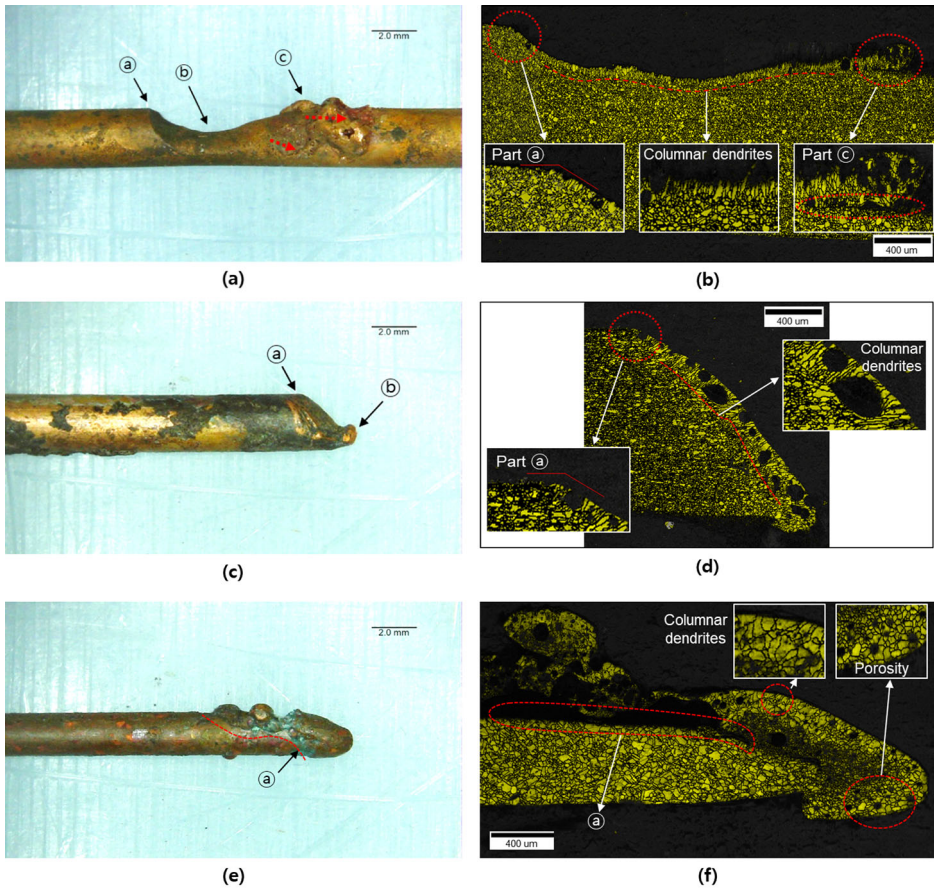


**Figure 18. Melting marks and cross-sectional microstructures collected from a fire site. (a) Fire-site melting mark-1; (b) Cross-sectional microstructures of melting mark-1; (c) Fire-site melting mark-2; (d) Cross-sectional microstructures of melting mark-2; (e) Fire-site melting mark-3; (f) Cross-sectional microstructures of melting mark-3.**

electromagnetic and arc repulsion forces, and were observed in the appearance of the contact short arc site.

#### **4. Short-circuited Arc Sites From Fire Sites**

Figure 18 shows melting marks and cross-sectional microstructures collected from a fire site in cooperation with the national forensic service (NFC). Figure 18a is similar to Figs. 8, 11, 14 and Line-A in Figs. 9 and 15a. Part (a) in Fig. 18a is in the ramp-edge form, and part (c) is in the covered form. Part (b) is the deepest part and is expected to be the location of the contact between wires. Figure 18b

shows the cross-sectional microstructure of Fig. 18a. In parts (a) and (c) of Fig. 18b, the ramp edge and covered form can be observed. In Fig. 18b, part (c) shows the covered shape that is solidified on the surface of the un-melted wire. In particular, the space is identified between the melting marks and surface of the un-melted wire to demonstrate the covered form. From part (a) to part (c), columnar dendrites are identified. The columnar dendrite and internal porosity are used to identify short-circuited arc site [16–21]. Figure 18c is similar to line-B in Fig. 9 and Line-A(1) in Fig. 15b. In part (a) of Fig. 17c, the ramp-edge form is formed, and a small bead is observed in part (b). Figure 18d shows the cross-sectional microstructure of Fig. 17c. Columnar dendrites are identified. In parts (a) of Fig. 18b, the ramp edge form can be observed. Figure 18e is similar to Line-B and Line-A(2) in Fig. 15. The melting mark in Fig. 18e shows a covered form along part (a). Figure 18f shows the cross-sectional microstructure of Fig. 18e. Columnar dendrites and internal porosity are identified in Fig. 18f. Part (a) in Fig. 18f shows the space between the molten and un-melted regions.

## **5. Conclusion**

We analysed the visual characteristics of short-circuited arc sites for on-site identification. The effect of the electromagnetic and arc repulsion forces acting to form arc sites was identified by analysing the shape of arc sites produced by experiments. The results showed that the arc repulsion and electromagnetic forces acted on the short-circuited arc site. In particular, when the electric wires were in contact in a row, the influence of the arc repulsion force acting in all directions was dominant, and when the electric wires were in contact in a vertical or parallel manner, the effect of the electromagnetic force appeared prominent. As a result of the analysis of the shape of the short-circuited arc site, three characteristics of the ramp-edge shape, the covered shape, and the concave shape were observed owing to the effects of the arc repulsion and electromagnetic forces, and it was confirmed that the molten bead could occur in the ramp edge shape. Moreover, the arc repulsion and electromagnetic forces affected the arc site, regardless of the core type of the copper wire used in our study. When the difference in voltages applied to the copper wires occurred, a difference in the short circuit current occurred, which could affect the extent of the arc site. When a short circuit occurred at a high ambient temperature, more contact area of the copper wire melted, and, in some cases, the contact area was separated.

Short-circuited arc sites formed from the melted wire because of the instantaneous high temperature in the micro-contact area. Subsequently, the melted copper wire moved by the forces acting on the contact part, demonstrating a common characteristic of being rapidly solidified by the temperature gradient to form its shape. The visual characteristics based on the generation principle can be used as the criteria for distinguishing short-circuited arc sites.

In this study, the effect of arc repulsion and electromagnetic forces was confirmed by analysing the appearance of short-circuited arc sites of a contact arc fabricated experimentally, and three characteristics were listed. Although not all

short-circuit molten marks at the fire site have these characteristics, it can provide additional information to assist in distinguishing short-circuit and flame-melt marks through visual examination at the fire site. In future, we plan to study arc sites due to a non-contact arc and analysis of the further characteristics of short-circuited arc sites through a large-scale experiment considering various situations that may occur at the fire site.

## **Funding**

This research was supported by the Korea Electrical Safety Corporation [Grant Number 2020-0101-18] and by and the National Research Foundation of Korea (NRF) [Grant Number 2021R1F1A1058389]. The funder had no role in the study design; in the collection, analysis or interpretation of data; in the writing of the report; or in the decision to submit the article for publication.

## **Data Availability**

The data related to this work can be obtained from the corresponding author upon reasonable request.

## **Code Availability**

Not applicable.

## **Declarations**

**Conflicts of interest** The author declare that they have no conflict of interest to disclose.

**Ethics Approval** Not applicable.

**Consent to Participate** Approval.

**Consent for Publication** Approval.

## **Open Access**

This article is licensed under a Creative Commons Attribution 4.0 International License, which permits use, sharing, adaptation, distribution and reproduction in any medium or format, as long as you give appropriate credit to the original

author(s) and the source, provide a link to the Creative Commons licence, and indicate if changes were made. The images or other third party material in this article are included in the article's Creative Commons licence, unless indicated otherwise in a credit line to the material. If material is not included in the article's Creative Commons licence and your intended use is not permitted by statutory regulation or exceeds the permitted use, you will need to obtain permission directly from the copyright holder. To view a copy of this licence, visit <http://creativecommons.org/licenses/by/4.0/>.

## References

1. National Fire Protection Association (2021) NFPA 921: Guide for fire and explosion investigations
2. Babrauskas V (2021) Electrical fires and explosions. Fire Science Publishers, New York
3. Bureau of alcohol, tobacco, firearms, and explosives, fire research laboratory, technical bulletin 001: visual characteristics of fire melting on copper conductor
4. Fire Investigation Section of Tokyo Fire Department (1971) Electrical fire cause and identification, p. 17
5. M. Benfer, D. Gottuk, (2014) Distinguishing between arcing and melting damage in electrical receptacles. Proc Int Symp Fire Investig Sci and Technol
6. Cameron N (2020) A methodology for the identification and interpretation of damage on electrical wiring. Fire Arson Investig 71(1):22–30
7. Xu L et al (2012) Forces of rails for electromagnetic. Appl Math Model 36(4):1465–1476. <https://doi.org/10.1016/j.apm.2011.09.036>
8. Su CC (2006) Mechanisms for the longitudinal recoil force in railguns based on the electromagnetic force. IEEE Trans Magn 42(9):2193–2195. <https://doi.org/10.1109/TMAG.2006.878010>
9. Ternan JG (1985) Equivalence of the Lorentz and Ampere force laws in magnetostatics. J Appl Phys 57:1743–1745. <https://doi.org/10.1063/1.334448>
10. Keshtkar A, Khorrami ZJ, Gharib L (2017) Comparison of inductance gradient and electromagnetic force in two types of railguns with two projectiles by finite-element method. IEEE Trans Plasma Sci 45(8):2387–2392. <https://doi.org/10.1109/TPS.2017.2716357>
11. Sadiku M (2018) Elements of electromagnetics. Oxford University, Oxford
12. Bizjak M, Kharin S, Nouri H (2002) Influence of vapour pressure on the dynamics of repulsion by contact blow-off. In proceeding of 21st conference electrical contacts, 268–275
13. Shea JJ, DeVault B, Chien Y (1994) Blow-open forces on double-breaker contacts. IEEE Trans Comp Hybrids Manufact Techol 17(1):32–38. <https://doi.org/10.1109/95.296365>
14. Zhou X, Theisen P (1998) Investigation of arcing effects during contact blow open process. In Proceedings of 44th IEEE Holm Conference Electrical Contacts, 100–108
15. Weinschenk C, Madrzykowski D, Courtney P (2019) Impact of flashover fire conditions on exposed energized electrical cords/cables. Fire Technol 56:959–991. <https://doi.org/10.1007/s10694-019-00915-8X>

16. Lee EP et al (2000) Study on discrimination between primary and secondary molten marks by DAS. Bull Jpn Association Fire Sci Eng 50(1):1–12. [https://doi.org/10.11196/kasai.50.1\\_1](https://doi.org/10.11196/kasai.50.1_1)
17. Lee EP et al (2002) Study on discrimination between primary and secondary molten marks using carbonized residue. Fire Safety J 37:353–368. [https://doi.org/10.1016/S0379-7112\(01\)00064-9](https://doi.org/10.1016/S0379-7112(01)00064-9)
18. Yun W, Xiaoming S (2014) Study on pores distribution laws in secondary short circuited melted beads of copper wires. Procedia Eng 84(2014):887–892. <https://doi.org/10.1016/j.proeng.2014.10.511>
19. Liu KH, Shih YH, Chen GJ, Chou JM (2015) Microstructural study on molten marks of fire-causing copper wires. Materials 8:3776–3790. <https://doi.org/10.3390/ma8063776>
20. Park J, Kang JH, Lee EP et al (2021) New approach to distinguish copper molten marks based on quantitative microstructure analysis using electron backscatter diffraction. Fire Technol 57:1667–1682. <https://doi.org/10.1007/s10694-020-01076-9>
21. Liu KH et al (2015) Microstructural study on oxygen permeated arc beads. J Nanomater . <https://doi.org/10.1155/2015/373861>

**Publisher's Note** Springer Nature remains neutral with regard to jurisdictional claims in published maps and institutional affiliations.